Arabian Journal of Chemistry (2021) **14**, 103404

King Saud University

Arabian Journal of Chemistry

www.ksu.edu.sa
www.sciencedirect.com

ORIGINAL ARTICLE

Annealing dependent synthesis of cyto-compatible nano-silver/calcium hydroxyapatite composite for antimicrobial activities

Arumugam Dhanesh Gandhi [a,*], K. Kaviyarasu [b,c,*], Nookala Supraja [d], Rajendran Velmurugan [e], Gunasekaran Suriyakala [f], Ranganathan Babujanarthanam [f], Yang Zang [g], Khantong Soontarapa [a,*], Khalid S. Almaary [h], Mohamed S. Elshikh [h], Tse-Wei Chen [i]

[a] *Department of Chemical Technology, Faculty of Science, Chulalongkorn University, Bangkok, Thailand*
[b] *UNESCO-UNISA Africa Chair in Nanosciences/Nanotechnology Laboratories, College of Graduate Studies, University of South Africa (UNISA), Muckleneuk Ridge, PO Box 392, Pretoria, South Africa*
[c] *Nanosciences African Network (NANOAFNET), Materials Research Group (MRG), IThemba LABS-National Research Foundation (NRF), 1 Old Faure Road, 7129, PO Box 722, Somerset West, Western Cape Province, South Africa*
[d] *Nanotechnology Laboratory, Institute of Frontier Technology, Regional Agricultural Research Station, Acharya N G Ranga Agricultural University, Tirupati 517 502, AP, India*
[e] *Department of Biochemistry, Faculty of Science, Chulalongkorn University, Bangkok, Thailand*
[f] *Nano and Energy Biosciences Laboratory, Department of Biotechnology, Thiruvalluvar University, Serkkadu, Vellore 632115, Tamil Nadu, India*
[g] *Qingdao Institute of Bioenergy and Bioprocess Technology, Chinese Academy of Science (CAS), China*
[h] *Department of Botany and Microbiology, College of Science, King Saud University, P.O. 2455, Riyadh 11451, Saudi Arabia*
[i] *Department of Materials, Imperial College London, London SW7 2AZ, United Kingdom*

Received 1 July 2021; accepted 24 August 2021
Available online 30 August 2021

* Corresponding authors.
E-mail addresses: dhaneshmsc@gmail.com (A.D. Gandhi), kavi@tlabs.ac.za (K. Kaviyarasu), Khantong.S@chula.ac.th (K. Soontarapa).
Peer review under responsibility of King Saud University.

Production and hosting by Elsevier

https://doi.org/10.1016/j.arabjc.2021.103404

KEYWORDS

Hydroxyapatite;
Ureolytic *Bacillus* sp.;
Synthetic urine;
Antibacterial activity;
Anticancer studies;
Brine shrimp assay

Abstract Crystalline hydroxyapatite were synthesized from synthetic/human urine through precipitation which were further doped with silver nanoparticle for effective biomedical application. The aim were to improve overall biological compatibility of the synthesized bone-graft material even in oncogenesis cases. The thermal calcinated material was characterized by several techniques including UV–vis, Laser Raman, Fourier transmittance infrared spectroscopy, X-ray diffraction analysis, Transmission Eelectron microscopy and X-ray fluorescence spectroscopy. The quantitative and qualitative analysis revealed that the synthesized material was highly crystalline and nanosized with majority of silver and phosphate components. The antibacterial, anticancer and invitro cytotoxicity of the synthesized material was evaluated with *Escherichia coli*, Hela cells and brine shrimp assay, respectively. The brine shrimp assay revealed that the synthesized material is compatible with biological system, whereas anticancer activity showed the application of the synthesized biomaterial in cancer treatment in which antibacterial activity adds more advantage on preventing the bone-graft from microbial attack.

1. Introduction

The reduction of natural resource and increasing amounts of biological waste has created much attention worldwide. To achieve the needs of energy and daily requirements. The waste material has been utilized to synthesize useful products by developing technology worldwide. Human being excretes 1–2 L of urine every day which is mainly contains urea, protein, sugar, and minerals such as potassium, sulphur, phosphorus, calcium, magnesium, and sodium. The estimated approximate urea content in human urine is 10–16 g/day (Mc Pherson and Ben-Ezra, 2011), which is naturally enter in human-plant nitrogen cycle nutrient in agricultural industries. In some countries, human urine is directly used as a bio-fertilizer for agricultural purpose (Johansson, 2000). Urea is a byproduct of protein degradation in human metabolism that enters the bloodstream and is eliminated through the urine. CO_2 gas has been collected and sequestered in human urine recently. As a substitute for CO_2 gas obtained from urine, biological activated ammonia can be employed as a resulting product of ammonia carbonate and ammonia bicarbonate (Chandrasekaran et al., 2014). Many studies have been conducted on ureolytic bacteria and calcium precipitating bacteria that have been isolated and identified from toilet dropping (Otterpohl, 2003). These bacterial species play an important role in converting urea into ammonia. The formation of ammonia enhances the pH of the medium as result of precipitation of calcite, struvite, and hydroxyapatite. Generally, the chemical precipitation of calcium carbonate is inclined by the factors such as nucleation site, calcium concentration, pH, and dissolved inorganic carbon in many natural environments (Krause et al., 2018). When compared to chemical precipitation, the rate of microbial precipitation was substantially faster. Biomineralization is the term for physiologically mediated precipitation. Bacterial calcite precipitation (BCP) is the generation of $CaCO_3$ by bacteria via urea hydrolysis. Natural, pollutant-free, and naturally porous, BCP is extremely valued. In the field of bone tissue engineering, calcium phosphate biomaterials have been identified as suitable scaffold candidates (Breme et al., 1995; Wilson and Mjor, 2000). In the precipitation of hydroxyapatite, several biocatalysts such as plant urease and bacterial urease enzyme are commonly used.

Hydroxyapatite is the ample mineral in human bones (Koch et al., 2007). Calcium hydroxyapatite is a bioactive molecule that helps the substrate assist bone regeneration. Hydroxyapatite is mostly employed in the biomedical field, namely bio-implant materials for orthopedic, dental, and maxillofacial surgery (Lin et al., 2000). A strong bone implant interface can be performed between the hydroxyapatite and bone due to its good biocompatibility. Despite their chemical and structural similarities, the bioactivity, and mechanical capabilities of synthetic hydroxyapatite (HA) are far lower than those of natural hard tissues. HA has good biocompatibility and osteoconductivity in cell growth and adhesion in osteoblasts (Samavedi et al., 2013). The development of phase pure ultra-fine hydroxyapatite powder has been noticed by several research to improve the mechanical strength and fracture toughness of HA ceramics (Suchanek and Riman, 2006). This bioactive hydroxyapatite was synthesized by several techniques includes hydrothermal (Chye et al., 2008; Sanosh et al., 2009), and chemical precipitation (Aoki, 1991). A little work has been done on the microbial synthesis of calcium hydroxyapatite as a biosynthesis material particularly to be used in bio-medical filed (Arciola et al., 2018). Furthermore, physical vapor deposition (PVD) and chemical vapor deposition (CVD) were utilized for coating the calcium hydroxyapatite with the implant substrate. In an implant many bacterial Infections were noticed in recent years which is major problem, to overcome this major drawback the antimicrobial compounds like silver were incorporate in the bone grafting material (Ciobanu et al., 2013). Recently (Tidaker, 2003) developed a silver doped hydroxyapatite nanomaterial which was found to be more toxic to bacteria and less effect on humans with optimum concentration of nanoparticles.

In the present study, ureolytic bacteria were isolated from toilet dropping and utilized to establish a bio-approach for the synthesis of hydroxyapatite. UV–visible spectroscopy (UV–Vis), X-ray diffraction (XRD), Zeta potential (DLS), Laser Raman (RMN), Transmission electron microscope (TEM), X-Ray fluorescence spectroscopy (XRF), and Fourier Transmission Infrared spectroscopy (FTIR) were used to char-

acterize the final product. The biogenic silver doped hydroxyapatite material had been evaluated by microbial resistance activity against gram negative *Escherichia coli* (*E. coli*) bacterial species, anticancer activity by HeLa Cells and toxicity by brine shrimp assay.

2. Materials and methods

2.1. Isolation and screening of ureolytic bacteria

The samples were collected from the toilet dropping from public toilet for isolation of ureolytic bacteria. Sterilized swab was dipped in sterile distilled water immediately and carried out to the laboratory within 6 h. To isolate bacterial colonies from the sample a pour plate technique was used. Urea base agar and nutrient agar medium was used for bacterial isolation and purification was followed from the sample details in the supplementary data as shown in *Fig. S1*.

2.2. Preparation of synthetic urine

Synthetic urine was prepared as outlined by (Webster et al., 2000). Synthetic urine is made up of the following ingredients (g/L) purchased from Sigma Aldrich, Mumbai: 0.651 g calcium chloride, 0.651 g magnesium chloride, 4.6 g sodium chloride, 2.8 g potassium dihydrogen phosphate, 2.3 g sodium sulphate, 1.6 g potassium chloride, 1.0 g ammonium chloride, 1.1 g creatinine, 10 g trypticase soya broth (or) tryptone in 1000 mL water followed by sterilization then 25 g of urea was added in *Fig. S2*.

2.3. Estimation of biogenic ammonia production

A total of 100 mL of synthetic urine was prepared, seeded with ureolytic bacterial culture, and kept at room temperature for three days. The pH of the medium was measured, and the enrichment of bacterial culture was checked for ammonia generation using the Indo phenol method (Miernik et al., 1991). The synthetic urine was collected and spun at 6000 rpm for 30 min (Dhandapani et al., 2020 Jun 1), and the supernatant was filtered through a membrane filter (0.2 M). The presence of ammonia in the filtrate solution was determined using the indophenol technique. The resulting sample was kept at room temperature for 30 min, and the absorbance was read at 625 nm using UV–vis (Thermo Scientific Evolution 201) to determine the ammonia concentration as shown in the supplementary *Fig. S2*.

2.4. Determination of pH

The ureolytic bacteria were introduced into synthetic urine and kept for 7 days at room temperature. The change in pH during ammonia production was measured using digital pH meter (Eutech Instruments pH 510 - as shown in the supplementary *Fig. S3* (Brundavanam et al., 2015).

2.5. Chemical oxygen demand (COD)

Digester solution was prepared by adding 1.02 g $K_2Cr_2O_7$ was added in 16.8 mL of concentrated H_2SO_4 which was diluted in 50 mL of Millipore water containing 3.34 g of $HgSO_4$, finally total volume was made up to 100 mL. Catalyst solution was made by dissolving 1.34 g of Ag_2SO_4 in 250 mL of concentrated H_2SO_4 and stirring constantly until a clear solution was obtained. The 1.5 mL of above said digester solution and catalysis solution 3.5 mL was mixed with 2.5 mL of sample. For comparative study of COD, three different samples were analyzed (Urea broth, Synthetic urine, and Human urine) and the mixture were kept in the COD digester for 2 h at 150 °C. Later the samples were analyzed in COD meter at 420 nm as shown in the supplementary *Fig. S4* (Reeta Mary et al., 2018).

2.6. Estimation of carbonate and bicarbonate (Alkalinity reaction)

The acid-base titration is suitable for alkalinity solution where the alkalinity is neutralized to acid pH by using 0.5 N HCl as burette solution. At acidic pH, the solution contains carbonate, bicarbonate, and hydroxide. These weak bases were volumetrically calculated using acid-base titrations using strong acids such as diluted H_2SO_4 and phenolphthalein (P) and methyl orange (MO) as an indicator. In the burette, standard acid was taken, and the sample was taken in the Erlenmeyer flask. The P indicator was introduced and titrated, and the reading was recorded as "P" when it reached the end point. Then MO indicator was added to the Erlenmeyer flask, and the titration was maintained until the end point was reached, which was labeled as "M". The nature and amount of bases present in the solution may be easily determined based on the titrated values of "P" and "M" (Tian et al., 2016). The result was calculated by using the following formula:

$$\text{Base} = \frac{P\text{or}M\text{value} \times \text{Normality of HCl} \times \text{mol.wt. of carbonate and bicarbonate}}{\text{Volume of sample}} \text{ (mg/L)}$$

2.7. Biogenic ammonia mediated synthesis of silver doped hydroxyapatite

Calcium acetate, biologically activated ammonia, disodium hydrogen phosphate and silver nitrate are used as base material for the synthesis of hydroxyapatite (Won et al., 2010). The filtered biogenic ammonia from synthetic urine of about 250 mL was taken and mixed with disodium hydrogen phosphate. The mixture was continuously stirred for 1 h and 0.1 mM silver nitrate was added and stirred for 1 h. Calcium acetate (4.72 g) was dissolved thoroughly in 20 mL of sterile distilled water before being added drop by drop to the solution. The mixture was then mixed and heated at 70 °C for 6 h, then exposed to sunlight for silver photo-reduction, before being cooled to room temperature then the mixture was spun for 30 min at 6000 rpm. To eliminate excess ammonia, calcium, and phosphate (CP) ions, the precipitate was rinsed with distilled water. CP-50 °C, CP-400 °C, and CP-800 °C were used to calcinate the precipitate at varied annealing temperatures of the sample.

2.8. Characterization studies

2.8.1. UV–vis spectral analysis

The UV–vis absorbance spectrum represents the characteristic absorbance of a given material. From 250 to 800 nm, the UV–vis spectrum of this solution was recorded in a Spectra 50

ANALYTIKJENA Spectrophotometer (UV-2450, SHIMADZU Spectrophotometer) (AlSalhi et al., 2016).

2.8.2. X-ray diffraction (XRD)

The XRD analysis of the fine powdered samples was utilized to identify the crystalline nature of the samples. The samples were scanned from 10° to 90°, 2θ with copper K α radiation (Ni filter) at a rating of 40 kV, 20 mA using a computer controlled XRD system (Bruker, JOEL Model JDX-8030). The 'peak search' and 'search match' tools incorporated within the software (PAnalytical-X'pert High score plus) were used to identify the peak (Supraja et al., 2018).

2.8.3. Dynamic light scattering (Zeta potential)

The size of the distributed nanoparticles was determined using the principle of dynamic light scattering (DLS) approach utilizing a Nanopartica (HORIBA, SZ-100) compact scattering spectrometer after the aqueous suspension of the generated nanoparticles was filtered via a 0.22 μL syringe driven filter unit (Supraja et al., 2017).

2.8.4. Laser Raman spectra

Laser Raman spectroscopy (Renishawinvia Raman Microscope) was used to determine the nature of the sample at various temperatures, using wavelengths of 500–1500 cm^{-1} and a 25-second exposure time (100% intensity) (RFS 100/S-Bruker, Inc., Karlsruhe, Germany, Matlab 6.0 software) (Supraja et al., 2020).

2.8.5. Transmission electron microscope (TEM)

The morphology of the hydroxyapatite crystals formed at 50 °C, 400 °C and 800 °C were gold sputtered for the conductivity of the sample and examined under TEM (TESCAN, equipment with Vega-3 software) (Devanesan et al., 2018).

2.8.6. Fourier transform infrared (FTIR) spectroscopic analysis

FTIR, which is commonly employed to detect the functional group of chemicals, was employed to characterize the biochemical changes in the solution. The FTIR spectrum was obtained in the 400–4000 cm^{-1} mid-IR region, with a spectral resolution of 4 cm^{-1} (Bruker, Tensor 27-model) (Supraja et al., 2016).

2.8.7. Antibacterial activity

The antibacterial activity was studied for silver doped hydroxyapatite and undoped hydroxyapatite material against the gram-negative *Escherichia coli* ATCC 10536 bacterial species by Disc Diffusion method by using nutrient medium (Bedi et al., 2012; Supraja et al., 2020).

2.8.8. Anticancer activity

The HeLa cells were grown in Dulbecco's modified eagle medium (DMEM) containing 0.1 mM sodium pyruvate, 10% fetal bovine serum with 1 mM non-essential amino acids and 0.5 mM L-glutamine maintained at 37 °C in an incubator with the supplementation of 5% CO_2. The grown HeLa cells were loaded in 96 well titer plates at the concentration 0.2×10^6 and supplied with the test samples and by increasing concentration and kept for a day. After one day, 20 μL of 5 mg/mL concentrated MTT solution was added and kept for 4 h continued to dissolve the MTT formazan by the addition of 200 μL DMSO. The control was maintained without addition of the test sample then the developed purple colour absorbance were recorded at 770 nm. The formed formazan in the control is designated as 100% viability. Based on the formation of MTT into insoluble formazan represents the cell viability (Supraja et al., 2018).

2.8.9. Brine shrimp assay

For hatching, Brine shrimp eggs were kept in filtered artificial seawater made by dissolving 30 g of sea salt in 1L of distilled water. After two days the eggs were hatched and mature to nauplii (larva) in the hatching container (small plastic container) half covered with the dark. After the larva is ready, the experiments were conducted by adding 10-brine shrimp larva in petri plates containing 5 mL of sea water and 5 mL of test sample. The experiments were triplicated and the 10 mL of the sea water with nauplii were maintained as control. Using the probit analysis the half lethal concentration was analysed by the confidence interval of 95%. The percentage mortality (%M) was obtained by dividing the number of dead nauplii by the total number of nauplii and multiplying by 100% (Supraja et al., 2015).

2.9. Statistical analysis

Student's *t*-test was used to examine the statistical significance of the experiments. For three corresponding measurements, all the results were represented as mean ± SD.

3. Results and discussion

3.1. Identification of bacteria

Urease test was used to classify organisms based on their ability to hydrolyze urea with Urease enzyme to identify ureolytic bacteria in a series of isolated single colony. The cultures were cultivated in urea broth medium with phenol red as a pH indicator. The positive bacteria used urea as a substrate and formed an alkaline environment in the presence of ammonia, which turned the phenol red into a deep pink color. The presence of urease enzyme and biochemical studies confirmed that the isolated microorganism as ureolytic *Bacillus* sp. (Fig. S1).

3.2. Production of ammonia

The isolated ureolytic *Bacillus* sp. was incubated in synthetic urine for 5 days at room temperature. Then the sample was withdrawn at regular time interval from the synthetic urine. The samples were filtered, centrifuged and the presence of ammonia was estimated by Indophenol blue method in UV spectrophotometer (Thermo Scientific Evolution 201) at 625 nm. The resultant production of ammonia was 9000 ppm on 3rd day of cultures in the medium shown in supplementary data (Fig. S2). The isolated ureolytic bacteria were inoculated into synthetic urine at initial pH 6.0. The production of ammonia was observed as the pH of the bacterium changed during its growth. The result of changes in pH was shown in supplementary data Fig. S3. The pH was gradually increased from pH 9.0 to pH 12.0 within 48 h. The COD was estimated in urea broth, synthetic urine and human urine

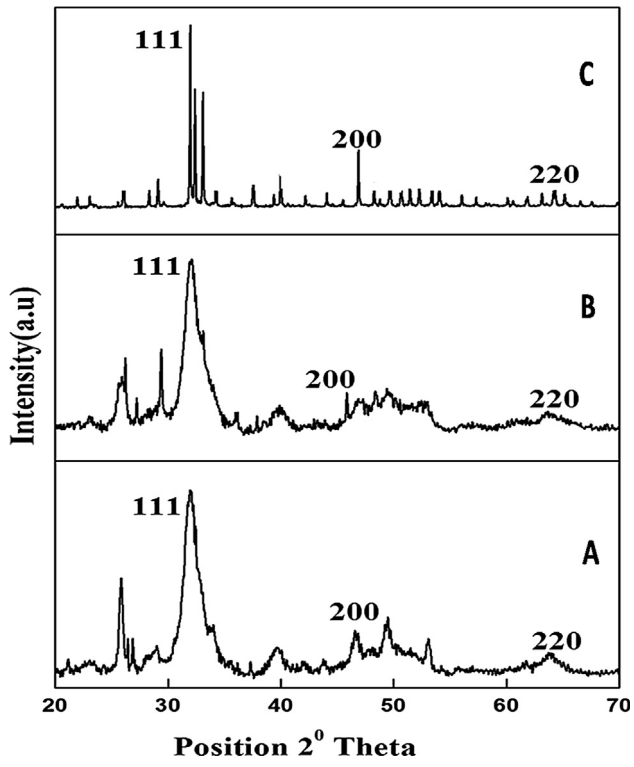

Fig. 1 X-ray diffraction pattern of silver doped hydroxyapatite at different temperatures (A-50 °C, B-400 °C and C-800 °C).

using standard procedure. The level of COD in synthetic urine was greater than the urea broth but less than the human urine, almost the level of COD in synthetic urine was approximately equal to human urine and the details are provided in supplementary data (Fig.S4). The cultured synthetic urine by titration. It was estimated that bacteria produced 12 mg/L carbonate and of 19.75 mg/L bicarbonate in synthetic urine as shown in the supplementary data's Table S1.

The isolated bacterial culture was introduced into the urease medium, which contains peptone and glucose, two necessary nutrients for a wide variety of bacteria. Potassium phosphate is a moderate buffer that prevents the medium from becoming alkaline due to peptone metabolism. When the media was below pH 8.4, phenol red indicated yellowish orange, and when the media was in the alkaline range, it signified red or pink. (pH 9–12). The urea hydrolysis of urea to ammonia by urease positive organisms changed the medium pH resulted in orange to pink. Urease catalyzes the hydrolysis of urea to produce ammonia and carbonate, which then hydrolyzes automatically to produce carbonic acid and another molecule of ammonia. The ureolytic bacterium which was isolated from toilet dropping was confirmed as *Bacillus sp* by biochemical test and it was inoculated in the synthetic urine to produce the ammonia. It was observed that 9000 ppm of ammonia was produced on third day which was in dissolved state in synthetic urine and combined with the carbonate and bicarbonate that was estimated by the alkalinity reaction.

The culture filtrate was rich in biogenic ammonia used for the synthesis of hydroxyapatite. Because of their chemical and structural similarities to the mineral phase of bone and tooth, calcium phosphate compounds have been explored for biomedical uses. Synthetic apatite's composition, physicochemical characteristics, crystal size, and shape are particularly sensitive to preparative conditions, and non-stoichiometric calcium deficient hydroxyapatite (HA) powder has occasionally produced. Silver is doped on the surface of calcium hydroxyapatite due to electrostatic contact. The previous research of (Supraja et al., 2018) states the roughness of the calcium hydroxyapatite is increased due to the deposition of the silver particles which result in enhanced cell proliferation.

3.3. Characterizations of silver deposited hydroxyapatite

The UV–vis absorption spectrum of the synthesized silver deposited hydroxyapatite sample at different temperatures is given in supplementary data Fig. S5. There is a maximum absorption peak at 470 nm was observed for the samples

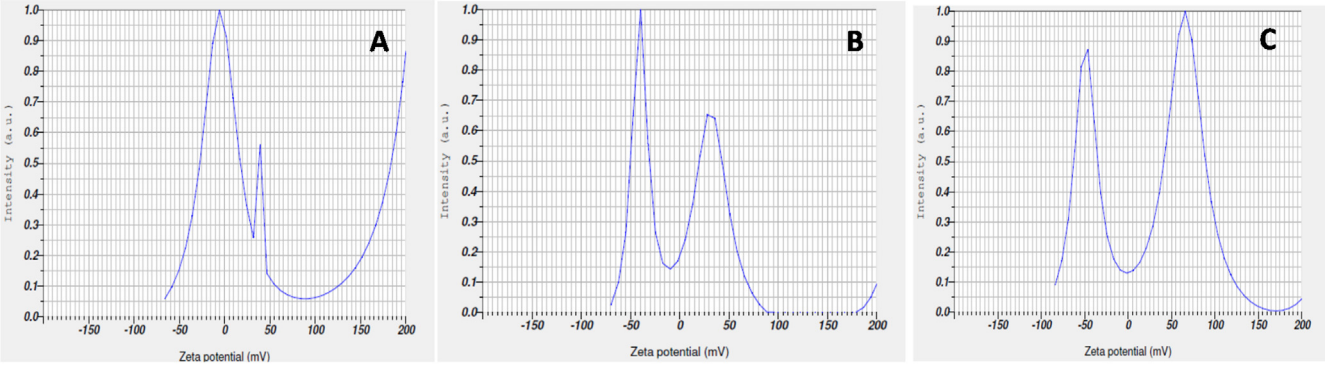

Fig. 2 Zeta potential study of silver doped hydroxyapatite at different temperatures (A-50 °C, B-400 °C and C-800 °C).

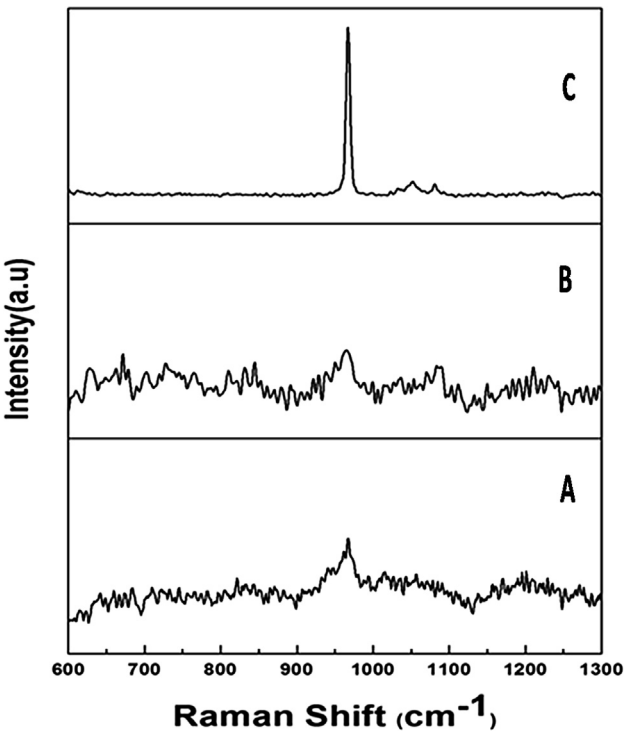

Fig. 3 Laser Raman spectral analysis of silver doped hydroxyapatite at different temperatures (A-50 °C, B-400 °C and C-800 °C).

prepared at 50 °C, 400 °C and 800 °C. The adsorption peak was gradually increased by increasing the temperature from 400 °C to 800 °C. This is an indication that $AgNO_3$ is reduced to Ag at higher temperature without organic or chemical reducing agents. The synthesized particle of ureolytic *Bacillus* sp. mediated hydroxyapatite was analyzed by XRD to know the nature of the particle. At 50 °C the particle was in amorphous state and at the 800 °C the particle was crystalline in nature and the peak at 26°, 29°, 31°, 32°, 33°, 34°, 37° and 40° theta showed the presence of hydroxyapatite Fig. 1. At 50 °C, only the broad peak at 32° appeared and then at 400 °C the peak at 26^0, 29^0, 37^0 and 40^0 got raised and all the linear peaks appeared at 800 °C which confirms the presence of the hydroxyapatite in crystalline nature. XRD of silver particles with one strong distinguishing peak at $2\theta = 37.2$ °C corresponds to the Braggs crystal faces of (1 1 1) and (2 0 0) (JCPDS # 04-0783) corroborating the characteristic of face-centered cubic structure. The zeta potential is a crucial characteristic in determining the hydrosol's dispersion state (nanoparticulate solution). It denotes that the overall charge that a particle obtains in each medium, as well as the charge present on the nanoparticles' surfaces, are responsible for the repulsive interactions that exist between them. If the minimum charge around the nanoparticles is −30 mV, the nanoparticles are said to be stable. At 50 °C, 400 °C, and 800 °C the silver doped hydroxyapatite had a zeta potential of 7.7 mV, -7.8 mV, and 11.1 mV respectively. An anionic charge on the surface of a composite material is shown in Fig. 2(a-c).

The existence of the PO_4^{3-} group is shown by the primary peak being elevated at 961 cm^{-1} in the laser Raman spectrum. The intensity of the peak at 50 °C was significantly lower than at 400 °C and 800 °C, which is attributable to the removal of the hydroxide and carbonate groups. At 800 °C, however, the disturbance of the peak was decreased by raising the temperature (Fig. 3). The size and shape of silver deposited hydroxyapatite nanoparticles were analyzed and shown by the TEM micrograph (Fig. 4). Individual silver particles as well as several aggregates are observed in the micrograph, that are spherical in shape and have an average particle size of 0.2 m.

The XRF spectrum of silver doped hydroxyapatite is shown in Fig. 5. The elemental maps for calcium (Ca), phosphor (P) and silver (Ag) was observed in which the highest peak was observed at Ca region followed by silver and P, respectively. FTIR spectra of silver doped hydroxyapatite is given in Fig. 6. The peaks at 3443 cm^{-1} and 2361 cm^{-1} were responsible to the asymmetrical stretching mode of O-H and C = O; an asymmetrical stretching of CH_2 was observed at 1450 cm^{-1}; the peaks at 1049 cm^{-1}, 866 cm^{-1} and 563 cm^{-1} were liable for to the asymmetrical stretching mode of O-H, C-C and C-H respectively. The peaks of 3443 cm^{-1} and

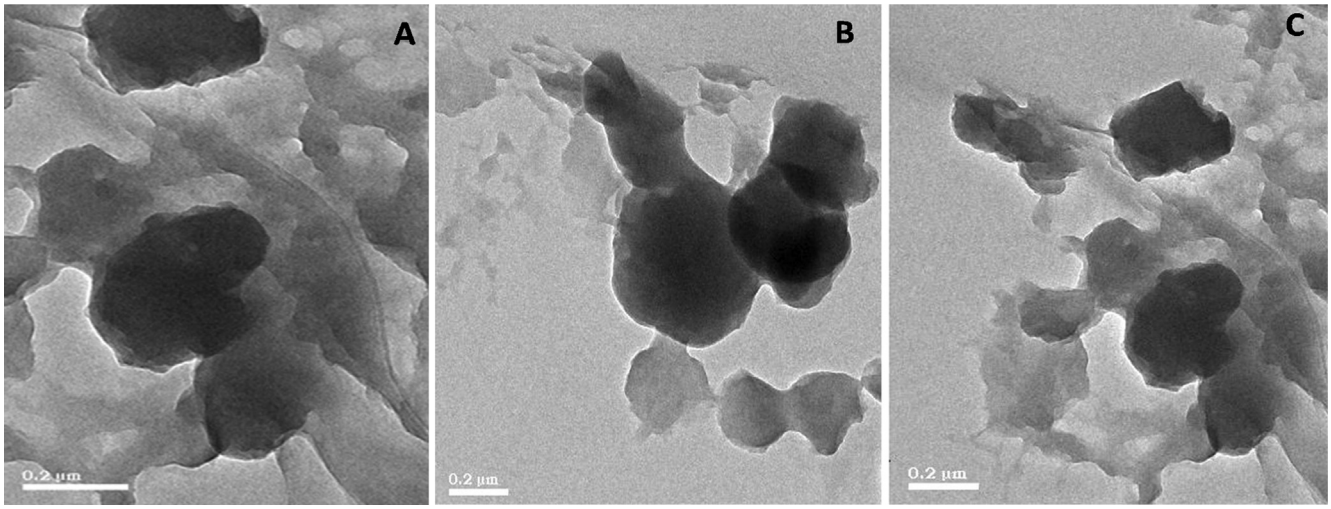

Fig. 4 Transmission electron microscopic analysis of silver doped hydroxyapatite at different temperatures (A-50 °C, B-400 °C and C-800 °C).

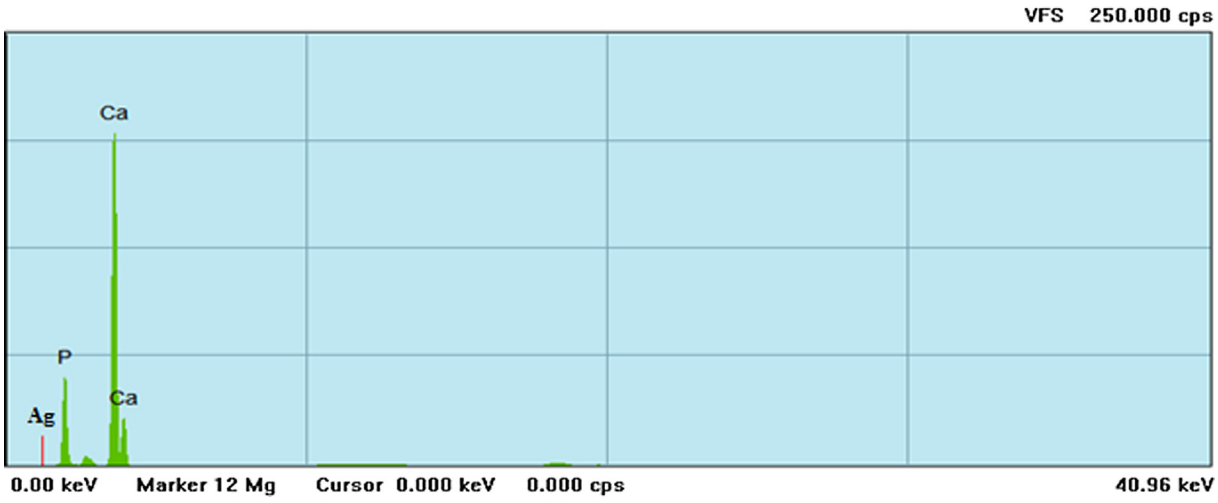

Fig. 5 X-ray fluorescence microscopic investigation of silver doped hydroxyapatite at 800 °C.

2361 cm^{-1} were present at 50 °C whereas these two peaks were not seen in 400 °C and 800 °C, which is due to the presence of H_2O absorption in the samples. The FTIR spectra obtained clearly showed the presence of calcium phosphate and carbonate groups, as well as hydroxyapatite.

3.4. Antibacterial activity

The study of antibacterial activity suggested that silver doped hydroxyapatite could inhibit the growth of bacteria *6* and the zone was formed in Sample A (50 °C), B (400 °C) and C (800 °C) and the zone was not formed in the control and A (Fig. 7). As a result, the nanoparticles of silver doped hydroxyapatite samples are placed closer to the bacteria, resulting in direct interaction between the bacteria and the silver nanoparticles. This is owing to the calcium particles' hydrophilic groups, which aid in the dispersion of the silver nanocomposite in aqueous solution. Bacteria (*E. coli*) easily interact with hydrophilic surfaces; as a result, bacteria may easily attach to the hydrophilic surface of the nanocomposite, where the silver particles of the composite could kill the bacteria (Supraja et al., 2015; Bauer et al., 19661966; Saritha et al., 2019; Bindu et al., 2019). Our results of antibacterial study clearly show that infection of the implant materials will be decreased.

3.5. Anticancer activity

The in-vitro cytotoxicity of the silver doped hydroxyapatite was evaluated against HeLa cell lines at different concentrations (Control and 10–50 μg/mL). The samples cytotoxicity analysis revealed a direct temperature response relationship, with cytotoxicity increasing as temperature rose (Fig. 8). The results demonstrated a considerable cytotoxicity against the HeLa cell lines. Silver deposited hydroxyapatite inhibited

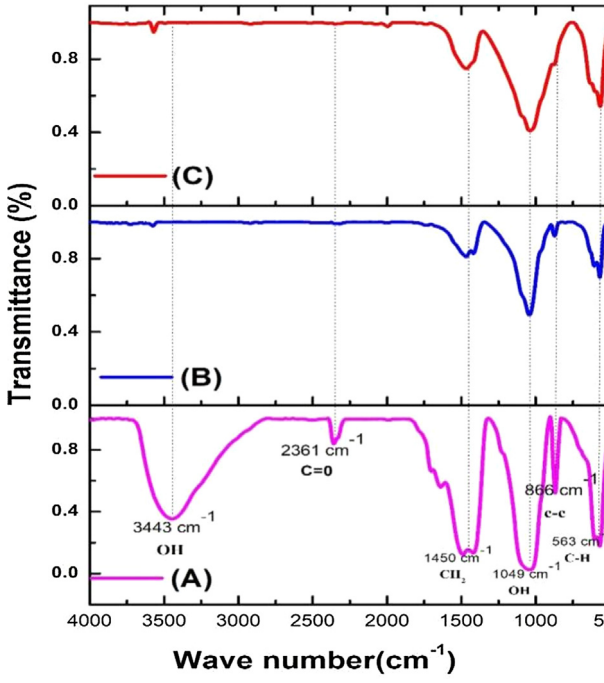

Fig. 6 FTIR analysis of silver doped hydroxyapatite at A-50 °C, B-400 °C and C-800 °C.

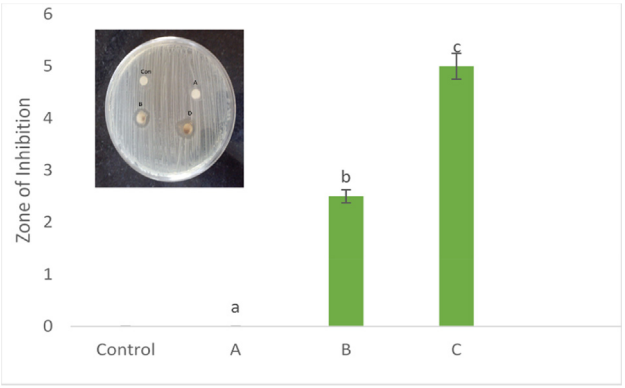

Fig. 7 Antibacterial efficacy of silver doped hydroxyapatite at different concentrations (Control-CHAP, A-50 °C, B-400 °C and C-800 °C). The different letters on each column indicates the significant difference.

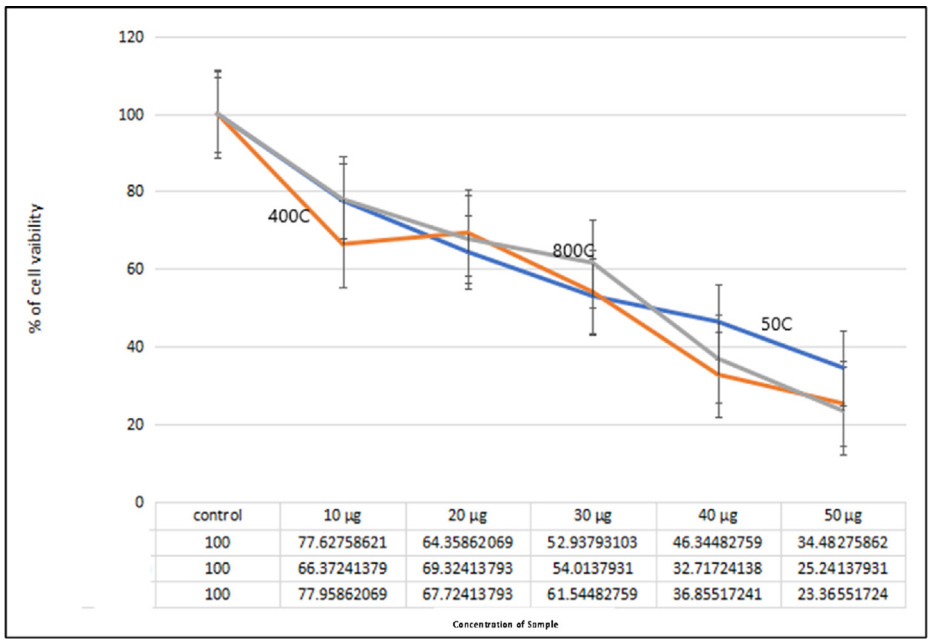

control	10 µg	20 µg	30 µg	40 µg	50 µg
100	77.62758621	64.35862069	52.93793103	46.34482759	34.48275862
100	66.37241379	69.32413793	54.0137931	32.71724138	25.24137931
100	77.95862069	67.72413793	61.54482759	36.85517241	23.36551724

Fig. 8 Anticancer efficacy of silver doped hydroxyapatite at different temperatures (Control, 50 °C, 400 °C and 800 °C).

HeLa cell proliferation significantly with an IC_{50} value of 30.9155 (124.6%) µg/mL of the concentration at 50 °C, whereas the IC_{50} value of 40.3786 (1947%) µg/mL of the concentration at 400 °C and IC_{50} value of 42.7488 (1014%) µg/mL at 800 °C respectively. Silver doped hydroxyapatite inhibited the proliferation of the cell line by less than 30% at the lowest concentration tested (10 g/mL). The existence of 50 g/mL of silver doped hydroxyapatite, drastically slowed the cell line's development (> 75%). When compared to the temperature, the 800 °C shown highest cytotoxicity effect. Nanoparticles deplete intracellular antioxidants causing cancer cell death according to a previous study (Supraja et al., 2020; Anand et al., 2017; Renuka et al., 2020).

3.6. Brine shrimp assay

The larvicidal activity of the silver doped hydroxyapatite tested on brine shrimp was weak. The test sample concentration was inversely proportional to the degree of lethality (Paramanantham et al., 2019; Paramanantham et al., 2019; Sairengpuii et al., 2020). The highest mortality of 40% was observed at 50 °C while, 400 °C and 800 °C does not show any mortality (Fig. 9). The lethality of silver doped hydroxyapatite is very moderately toxic (active) if the LC50 value is less than 1000 mg/mL, but non-toxic (inactive) if the LC50 value is higher than 1000 mg/mL, indicating the existence of significant cytotoxicity (Bauer et al., 19661966). The ureolytic bacterial species are converted ammonia and carbonic acids from synthetic urine by urease and ammonia production as described by our previous report (Dhandapani et al., 2020). The culture filtrate was rich in biogenic ammonia used for the synthesis of hydroxyapatite and chemical ammonia was also used for the synthesis for comparative study. Calcium phosphate compounds have been studied for biomedical applications due to chemical and structural similarity to the mineral phase of bone and tooth. The composition, physico-chemical properties, crystal size and morphology of synthetic apatite are extremely sensitive to preparative conditions and sometimes it resulted into non-stoichiometric calcium deficient hydroxyapatite (HA) powder (Nagasundari et al., 2021; Mani et al., 2021). In this study, ureolytic bacteria were isolated and developed ureolytic bacteria mediated hydroxyapatite and doped with silver nanoparticles. The silver doped hydroxyapatite was characterized and its antibacterial activity against the pathogenic microorganism of *E. coli* was evaluated (Badineni et al., 2021). The present results (UV, FTIR, XRD, DLS, TEM) was in good in accordance with previous reports regarding silver doped HAp material preparation by various methods (Shi et al., 2015; Stanić et al., 2011; Vukomanović et al., 2015). The

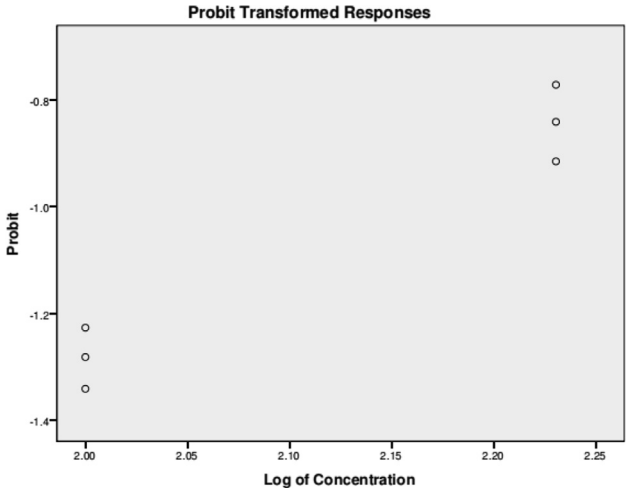

Fig. 9 Probit analysis brine shrimp assay of silver doped hydroxyapatite.

antibacterial activity of the silver doped hydroxyapatite was found to be substantially higher in 20 mg concentration than 10 mg the characterization studies were carried on 20 mg concentration of silver doped hydroxyapatite these doped hydroxyapatite can be used for bone grafting and Biofertilizers purposes the previous investigators have also proposed several mechanisms on antibacterial activity by AgNPs [30, 34 & 39]. The present result was indicated that our synthesized material has good cell viability for HeLa cell lines. Besides, the antibacterial activity exhibited by our material was also found to prevent bacterial infection (Mani et al., 2021; Mani et al., 2021).

4. Conclusions

Microbial synthesis of hydroxyapatite from synthetic/human urine is an eco-friendly and non-toxic process for the synthesis of bone-graft material. The silver doping improves the stability, in which the annealing condition was found to control the characteristics of silver doped hydroxyapatite. Such stable crystalline product can be more resistant to eradication. On the other hand, the biocompatibility studies on shrimp showed that the silver doped hydroxyapatite is more compatible. The resulting material also exhibiting antimicrobial activity which reduces the use of antibiotics. Results obtained in this study demonstrated that silver doped hydroxyapatite nanoparticles may offer an effective alternative to antibiotic treatments, exhibiting a specific spectrum of antimicrobial activity. Calcium hydroxyapatite (HP, $Ca_{10}(PO_4)_6(OH)_2$) is the main mineral constituent of a human bone bio-implant materials such as orthopedic, dental, treatment of wounds, burns infections, wound dressings, coating of bone prostheses and maxillofacial application. Moreover, the synthesized product was active against HeLa cells which can be beneficial in implantation of bone-graft to the cancer patient.

Acknowledgement

Arumugam Dhanesh Gandhi is grateful to the second century fund (C2F) Chulalongkorn University for the providing the Postdoctoral fellowship grant. Also, the authors extend appreciation to the Researchers supporting project number (RSP-2021/189), King Saud University, Riyadh, Saudi Arabia.

Appendix A. Supplementary data

Supplementary data to this article can be found online at https://doi.org/10.1016/j.arabjc.2021.103404.

References

Mc Pherson, R.A., Ben-Ezra, J., Basic examination of urine. (2011) "In: Mc Pherson, R.A., Pincus MR, eds Henry's clinical Diagnosis and Management by Laboratory methods. 22nd ed. Philadelphia, Pa: Elsevier Saunders", Chapter 28.

Johansson, M. (2000) "Urine separation closing the nutrient cycle. Final report on the R&D project: Source-separated human urine a future source of fertilizer for agriculture in Stockholmregion", Stockholm Water, 1-40.

Chandrasekaran, K., Selvaraj, R., Maruthamuthu, S., Kandasamy, S., Rajagopal, Gopala krishnan, 2014. Biogenic ammonia for CO_2 capturing and electrochemical conversion into bicarbonate and formate. J of CO2 Utiliz 6, 53–61.

Otterpohl, R., 2003. "New technological development in ecological sanitation. Paper published in Conf. In: Proceedings: 2nd International Symposium on ecological sanitation, pp. 455–462.

Krause, S., Liebetrau, V., Löscher, C.R., Böhm, F., Gorb, S., Eisenhauer, A., Treude, T., 2018 Dec. (2018) Marine ammonification and carbonic anhydrase activity induce rapid calcium carbonate precipitation. Geochim. Cosmochim. Acta 15 (243), 116–132.

Breme, J., Zho, Y., Groh, L., 1995. Development of titanium alloy suitable for optimized coating with hydroxyapetatite. Biomatrials 16, 239–244.

Wilson, N.H.F., Mjor, J., 2000. The teaching of class I and class II direct composite restorations in European dental school. J Dent 28, 15–20.

Koch, C.F., Johnson, S., Kumar, D., Jelinek, M., Chrisey, D.B., Doraiswamy, A., Jin, C., Narayan, R.J., Mihailescu, I.N., 2007. Pulsed laser deposition of hydroxyapatite thin films. Mater Sci and Eng: C 27 (3), 484–494.

Lin, Feng-Huei, Chun-Jen, Liao, Ko-Shao, Chen, Jui-Sheng, Sun, 2000. Thermal reconstruction behavior of the quenched hydroxyapatite powder during reheating in air. Mater. Sci. Eng., C 13 (1-2), 97–104.

Samavedi, Satyavrata, Whittington, Abby R., Goldstein, Aaron S., 2013. Calcium phosphate ceramics in bone tissue engineering: a review of properties and their influence on cell behavior. Acta Biomater. 9 (9), 8037–8045.

Suchanek, Wojciech L., Riman, Richard E., 2006. Hydrothermal synthesis of advanced ceramic powders. Adv Sci Technol 45, 184–193.

Chye, S., Loo, J., Siew, Y.E., Ho, S., Boey, F.Y.C., Ma, J., 2008. Synthesis hydrothermal treatment of nanostructured hydroxyapatite of controllable sizes. Jr of Mat Sci : Mate in medi 19, 1389–1397.

Sanosh, K.P., Chu, Min-Cheol, Balakrishnan, A., Kim, T.N., Cho, Seong-Jai, 2009. Preparation and characterization of nanohydroxyapatite powder using sol–gel technique. Bull. Mater. Sci 32 (5), 465–470.

Aoki, H. (1991) "Science and Medical Applications of Hydroxyapatite, Tokyo, Takayama Press System Centre, JAAS, Tokyo", 165.

Arciola, Carla Renata, Campoccia, Davide, Montanaro, Lucio, 2018. Implant infections: adhesion, biofilm formation and immune evasion. Nat. Rev. microbial. 16 (7), 397–409.

Carmen Steluta Ciobanu., Simona Liliana Iconaru., Ariana Carmen Chiriuc., Adrian Costescu., Philippe Le Coustumer., Daniela Predoi. (2013) "Synthesis and Antimicrobial Activity of Silver-Doped Hydroxyapatite", Nanop Article ID 916218.

Tidaker, P. (2003) "Life Cycle Assessment of grain production using source-separated human urine and mineral fertilizer", SLU, Dept. of Agricultural Engineering, Uppsala, Sweden. Report 251.

Webster, T.J., Ergun, C., Doremus, R.H., Siegel, R.W., Bizios, R., 2000. Enhanced functions of osteoblasts onnano phase ceramics. Biomaterials 21, 1803–1810.

Miernik, J.H., Shah, B.H., McGriff, C.F., 1991. "Waste Water Processing Technology for Space Station Freedom: Comparative Test Data Analysis, SAE Technical Paper Series No. 911416, 66.

Dhandapani, P., Devanesan, S., Arulprakash, A., AlSalhi, M.S., Paramasivam, S., Rajasekar, A., 2020 Jun 1. (2020) Bio-approach synthesis of nanosilver impregnation on calcium hydroxyapatite by biological activated ammonia from urinary waste. Arabian J. Chem. 13 (6), 5878–5889.

Brundavanam, Sridevi, Poinern, Gérrard Eddy Jai, Fawcett, Derek, 2015. Synthesis of a hydroxyapatite nanopowder via ultrasound irradiation from calcium hydroxide powders for potential biomedical applications. Nanoscience and Nanoengineering 3 (1), 1–7.

Reeta Mary, I., Sonia, S., Navadeepthy, D., Mangalaraj, D., Viswanathan, C., Ponpandian, N., 2018. Surfactant-free solvothermal synthesis of Hydroxyapatite nested bundles for the effective photodegradation of cationic dyes. J. Phys. Chem. Solids 116, 180–186.

Tian, Bo, Chen, Wei, Dong, Yufeng, Marymont, John V., Lei, Yong, Ke, Qinfei, Guo, Yaping, Zhu, Zhenan, 2016. Silver nanoparticle-loaded hydroxyapatite coating: structure, antibacterial properties, and capacity for osteogenic induction in vitro. RSC Adv. 6 (11), 8549–8562.

Won, Ji Yeong, Min, Junhong, Park, Jung-Hwan, 2010. Bacteria adsorption on hydrophilic surfaces for the, sensitive detection of pathogenic bacteria using a single tube chamber system. Biosens. Bioelectron 26 (4), 1763–1767.

AlSalhi, M.S., Devanesan, S., Alfuraydi, A.A., Vishnubalaji, R., Munusamy, M.A., Murugan, K., Benelli, G., 2016. Green synthesis of silver nanoparticles using Pimpinella anisum seeds: antimicrobial activity and cytotoxicity on human neonatal skin stromal cells and colon cancer cells. Int. J. Nanomed. 11, 4439.

Supraja, N., Dhivya, J., Prasad, T.N.V.K.V., David, E., 2018. Synthesis, characterization and dose dependent antimicrobial and anticancerous efficacy of phycogenic (Sargassum muticum) silver nanoparticles against Breast Cancer Cells (MCF 7) cell line. Advances in nano research 6 (2), 183.

Supraja, N., Avinash, B., Prasad, T.N.V.K.V., 2017. Nelumbo nucifera extracts mediated synthesis of silver nanoparticles for the potential applications in medicine and environmental remediation. Advances in nano research 5 (4), 373.

Supraja, N., Kishore, B., Rajasekhar, K.K., Padmavathamma, M., 2020. Synthesis of Carica Papaya (Leaf, Peel and Seed) Extracts Mediated Ag Nanoparticles for Industrial and Medical Applications *Chem*. Sci. Eng. Res. 2 (5), 29–39.

Devanesan, Sandhanasamy, AlSalhi, Mohamad S, Balaji, Radhakrishnan Vishnu, Ranjitsingh, Amirtham Jacob A, Ahamed, Anis, Alfuraydi, Akram A, AlQahtani, Fulwah Y, Aleanizy, Fadilah S, Othman, Ahmed H, 2018. Antimicrobial and cytotoxicity effects of synthesized silver nanoparticles from Punica granatum peel extract. Nanoscale Res. Lett. 13 (1). https://doi.org/10.1186/s11671-018-2731-y.

Supraja, N., Prasad, T.N.V.K.V., Krishna, T.Giridhara, David, E., 2016. Synthesis, characterization, and evaluation of the antimicrobial efficacy of Boswellia ovalifoliolata stem bark-extract-mediated zinc oxide nanoparticles. Applied Nanoscience 6 (4), 581–590.

Bedi, Rajwant S., Cai, Rui, O'Neill, Cory, Beving, Derek E., Foster, Stephen, Guthrie, Sean, Chen, Wilfred, Yan, Yushan, 2012. Hydrophilic and antimicrobial Ag-exchanged zeolite a coatings: a year-long, durability study and preliminary evidence for their general microbiocidal efficacy to, bacteria, fungus and yeast. Micropor. Mesopor. Mater 151, 352–357.

Supraja, N., Kishore, B., Rajasekhar, K.K., Padmavathamma, M., 2020. Synthesis of Carica Papaya (Leaf, Peel and Seed) Extracts Mediated Ag Nanoparticles for Industrial and Medical Applications. Chem. Sci. Eng. Res. 2 (5), 29–39.

Supraja, N., Dhivya, J., Prasad, T.N.V.K.V., Synthesis, David E., 2018. Characterization and Dose Dependent Antimicrobial and Anticancerous Efficacy of Phycogenic (Sargassum Muticum) Silver Nanoparticles against Breast Cancer Cells (MCF 7) Cell Line. Adv. Nano Res. 6, 183.

Supraja, N., Prasad, T.N.V.K.V., David, E., 2015. Synthesis, characterization and antimicrobial activity Of the micro/nano structured biogenic silver doped calcium phosphate. Appl Nanosci. https://doi.org/10.1007/s13204-015-0409-7.

Bauer, A.W., Kirby, M.M., Sheriss, J.C., Trunk, M. (1996) "Antibiotic susceptibility testing by a standardized single disk method", Am J Clin Pathol, 45, 493-496.

Dhandapani, Perumal, Prakash, Arumugam Arul, AlSalhi, Mohamad S., Maruthamuthu, Sundaram, Devanesan, Sandhanasamy, Rajasekar, Aruliah, 2020. Ureolytic bacteria mediated synthesis of hairy ZnO nanostructure as photocatalyst for decolorization of dyes. Mater. Chem. Phys. 243, 122619. https://doi.org/10.1016/j.matchemphys.2020.122619.

Shi, Chao, Gao, Jianyong, Wang, Ming, Fu, Jingke, Wang, Dalin, Zhu, Yingchun, 2015. Ultra-trace silver-doped hydroxyapatite with non-cytotoxicity and effective antibacterial activity. Mater. Sci. Eng., C 55, 497–505.

Stanić, Vojislav, Janaćković, Djordje, Dimitrijević, Suzana, Tanasković, Sladjana B., Mitrić, Miodrag, Pavlović, Mirjana S., Krstić, Aleksandra, Jovanović, Dragoljub, Raičević, Slavica, 2011. Synthesis of antimicrobial monophase silver-doped hydroxyapatite nanopowders for bone tissue engineering. Appl. Surf. Sci. 257 (9), 4510–4518.

Vukomanović, Marija, Repnik, Urška, Zavašnik-Bergant, Tina, Kostanjšek, Rok, Škapin, Srečo D., Suvorov, Danilo, 2015. Is nano-silver safe within bioactive hydroxyapatite composites? ACS Biomater. Sci. Eng. 1 (10), 935–946.

Saritha, V., Paul, A., Mariadhas Valan, A., Abdullah, Naif, 2019. Al., Abdul Kareem, M.G., Kaviyarasu, K., Balasubramani, R., Soon Woong, C., Arokiyaraj, S. Rapid biosynthesis and characterization of silver nanoparticles from the leaf extract of Tropaeolum majus L. and its enhanced in-vitro antibacterial, antifungal, antioxidant and anticancer properties. J. Photochem. Photobiol., B 191, 65–74.

Bindu, T., Vithiya, B., Prasad, T., Mohamed, S.B., Maria Magdalane, C., Kaviyarasu, K., Maaza, M., 2019. Antioxidant and Photocatalytic Activity of Aqueous Leaf Extract Mediated Green Synthesis of Silver Nanoparticles Using Passiflora edulis f. flavicarpa. J. Nanosci. Nanotechnol. 19 (5), 2640–2648.

Anand, K., Kaviyarasu, K., Muniyasamy, Sudhakar, Roopan, Selvaraj Mohana, Gengan, R.M., Chuturgoon, A.A., 2017. Biosynthesis of Silver Nanoparticles Using Agroforestry Residue and Their Catalytic Degradation for Sustainable Waste Management. J. Cluster Sci. 28 (4), 2279–2291.

Renuka, R., Devi, K.Renuka, Sivakami, M., Thilagavathi, T., Uthrakumar, R., Kaviyarasu, K., 2020. Biosynthesis of silver nanoparticles using Phyllanthus emblica fruit extract for antimicrobial application. Biocatalysis and Agricultural Biotechnology 24, 101567. https://doi.org/10.1016/j.bcab.2020.101567.

Nagasundari, S.M., Muthu, K., Kaviyarasu, K., Al Farraj, D.A., Alkufeidy, R.M., 2021. Current trends of Silver doped Zinc oxide nanowires photocatalytic degradation for energy and environmental application. Surf. Interfaces 23, 100931.

Mani, M., Pavithra, S., Mohanraj, K., Kumaresan, S., Alotaibi, Saqer S., Eraqi, Mostafa M., Gandhi, Arumugam Dhanesh, Babujanarthanam, Ranganathan, Maaza, M., Kaviyarasu, K., 2021. Studies on the spectrometric analysis of metallic silver nanoparticles (Ag NPs) using Basella alba leaf for the antibacterial activities. Environ. Res. 199, 111274. https://doi.org/10.1016/j.envres.2021.111274.

Badineni, V., Maseed, H., Arla, S.K., Yerramala, S., Naidu, B.V.K., Kaviyarasu, K., 2021. Effect of PVA/PVP protective agent on the formation of silver nanoparticles and its photocatalytic and antimicrobial activity. Mater. Today:. Proc. 36, 121–125.

Mani, M., Mohammad, K.O., Selvaraj, S., Ram Kumar, A., Kumaresan, S., Azhaguchamy, M., Kaviyarasu, K., Mohamed, A.El., Yahya, B.E., Khalid, S.A., Bander Mohsen, A., Almunqedhi, M.S., 2021. A novel biogenic Allium cepa leaf mediated silver nanoparticles for antimicrobial, antioxidant, and anticancer effects on MCF-7 cell line. Environ. Res. 198, 111199.

Mani, M., Harikrishnan, R., Purushothaman, P., Pavithra, S., Rajkumar, P., Kumaresan, S., Al Farraj, Dunia A., Elshikh, Mohamed Soliman, Balasubramanian, Balamuralikrishnan, Kaviyarasu, K., 2021. Systematic green synthesis of silver oxide nanoparticles for antimicrobial activity. Environ. Res. 202, 111627. https://doi.org/10.1016/j.envres.2021.111627.

Paramanantham, P., Anju, V.T., Sruthil Lal, S.B., Alok, S., Siddhardha, B., Kaviyarasu, K., Mohammed, A., Turki, M.S., Asad, Syed, 2019. Synthesis and antimicrobial photodynamic effect of methylene blue conjugated carbon nanotubes on E. coli and S. aureus. Photochem. Photobiol. Sci. 18 (2), 563–576.

Paramanantham, P., Asha, P.A., Alok, S., Busi, S., Kaviyarasu, K., Needa, A.B., Turki, M.S., Asad, S., 2019. Antimicrobial photodynamic activity of toluidine blue encapsulated in mesoporous silica nanoparticles against Pseudomonas aeruginosa and Staphylococcus aureus. Biofouling 35 (1), 89–103.

Sairengpuii, H., Kasinathan, K., Busi, S., 2020. Evaluation of Toxicity of Nanoparticles Using Brine Shrimp. Model Organisms to Study Biological Activities and Toxicity of Nanoparticles, Springer Ed., 401–415